Two cationic iron-based crystalline porous materials for encapsulating and sustained release of 5-fluorouracil

Xi-yu Sun[a], Hong-jing Zhang[a], Qian Sun[*a] and En-qing Gao[b]

Department of chemistry, School of Chemistry and Molecular Engineering, East China Normal University, Shanghai 200241, P. R. China;
Email: xsun@chem.ecnu.edu.cn

1. The synthesis and characterization of materials.

Terephthalic acid (H_2BDC) (34.8 mg), 2, 4, 6-tris(4-pyridyl)-1,3,5-triazine (TPT) (21.9 mg) and $Fe(ClO_4)_3 \cdot H_2O$ (78.3 mg) were added to 5mL DMF according to the molar ratio of 2:1:1, sonicated for 20 min until fully dissolved. Then transfer the solution to a reaction kettle heated in an oven at 120° C for five days. The temperature was slowly cooled down to obtain yellow microcrystalline. Elemental analysis (%) Calcd for CPM-83 $(Fe_3O(BDC)_3(TPT)](ClO_4)$: C, 46.38; H, 2.22; N, 7.73. Found: C, 45.67; H, 3.34; N, 7.44. Elemental analysis (%) for CPM-85, according to the formula of $[Fe_3O(BPDC)_3(TPT)](ClO_4)(DMF)$: calcd C, 54.47; H, 3.12; N, 7.06. Found: C, 53.95; H, 3.37; N, 7.63.

2. The characterization of materials.

2.1 X-ray powder diffraction

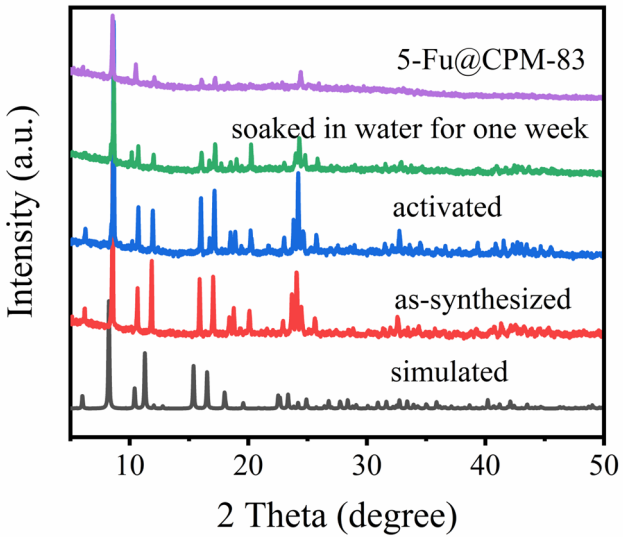

Figure S1 X-ray powder diffraction of CPM-83, activated CPM-83, CPM-83 soaked in water for one week, 5-Fu@CPM-83

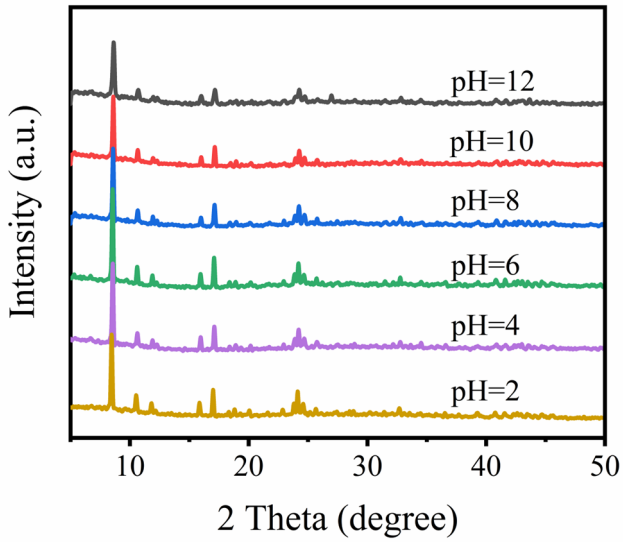

Figure S2 X-ray powder diffraction of CPM-83 in different pH solutions

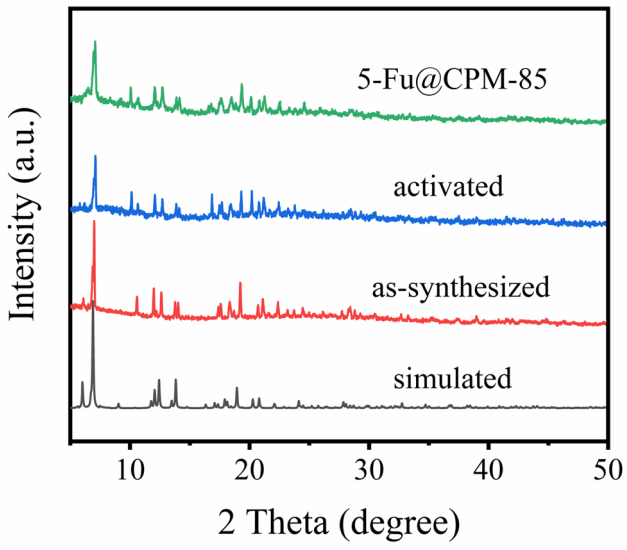

Figure S3 X-ray powder diffraction of CPM-85, activated CPM-85 and 5-Fu@CPM-85

2.2 Scanning Electron Microscope

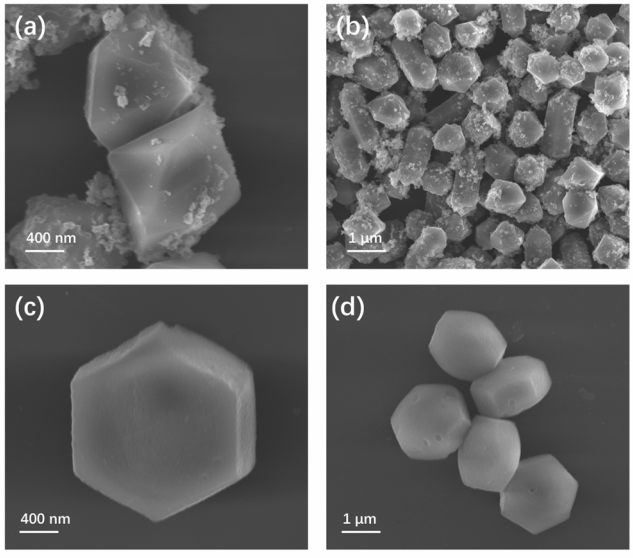

Figure S4 Scanning Electron Microscope of CPM-83 (a) (b), CPM-85 (c) (d)

2.3 Thermogravimetric analysis

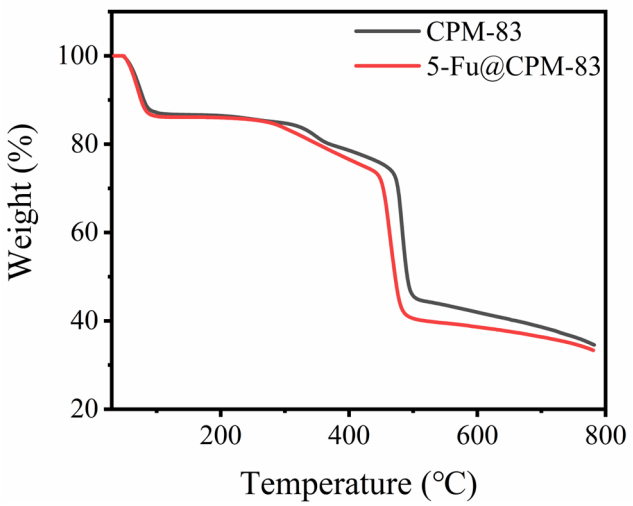

Figure S5 Thermogravimetric analysis of CPM-83 and 5-Fu@CPM-83

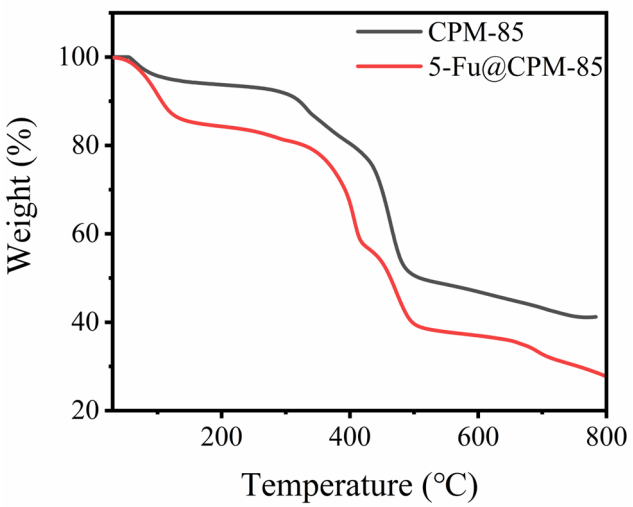

Figure S6 Thermogravimetric analysis of CPM-85 and 5-Fu@CPM-85

2.4 Infrared spectra characterization

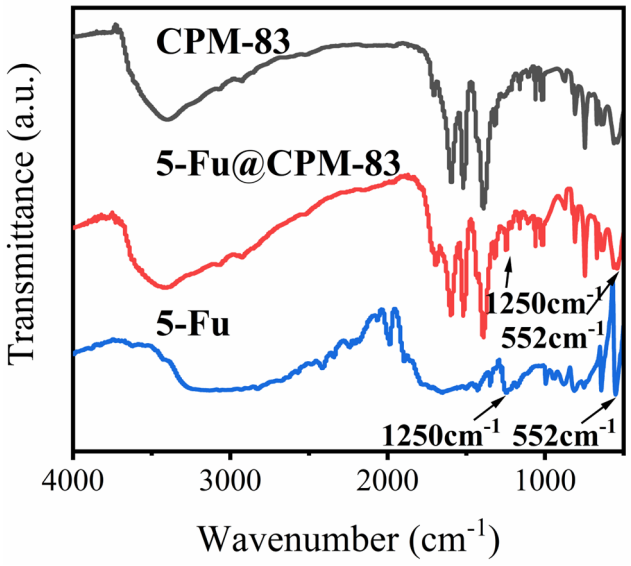

Figure S7 Infrared spectra of 5-Fu, CPM-83, 5-Fu@CPM-83

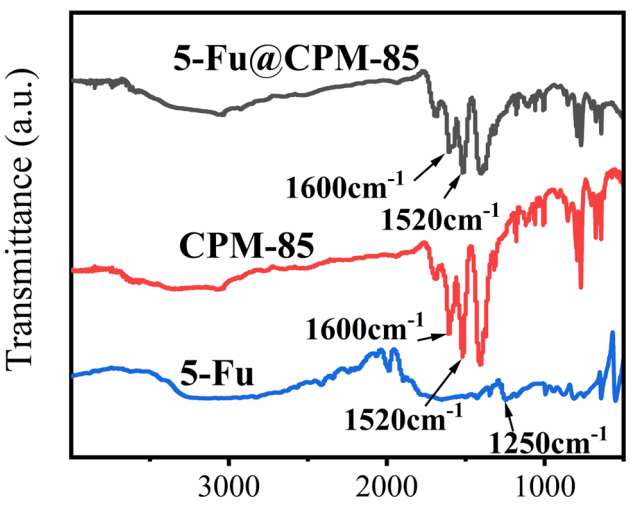

Figure S8 Infrared spectra of 5-Fu, CPM-85, 5-Fu@CPM-85

3. Standard curve of 5-Fu.

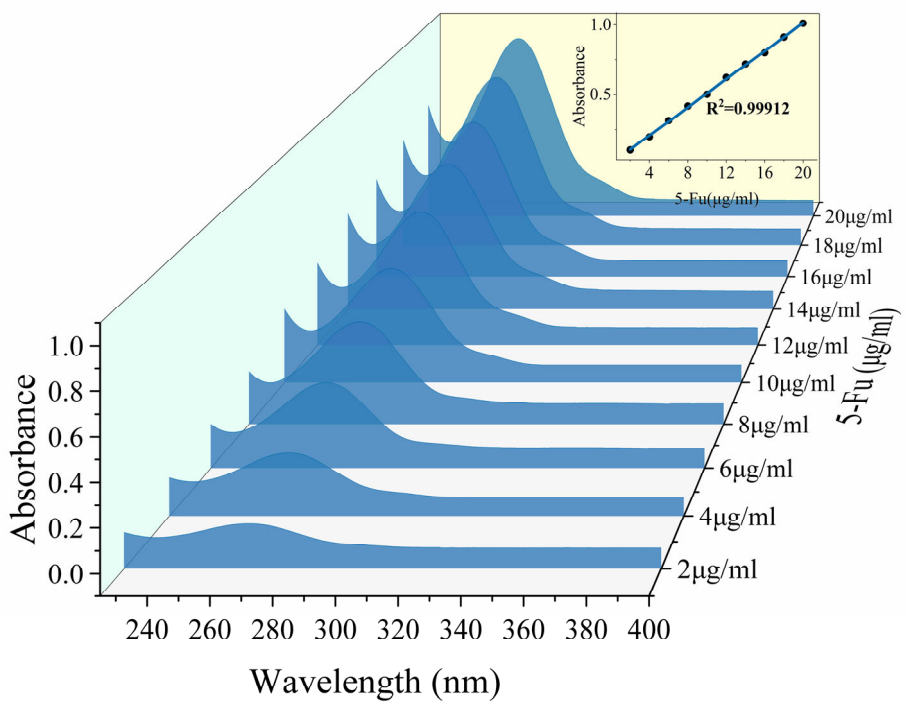

Figure S9 Standard curve of 5-Fu in PBS solution

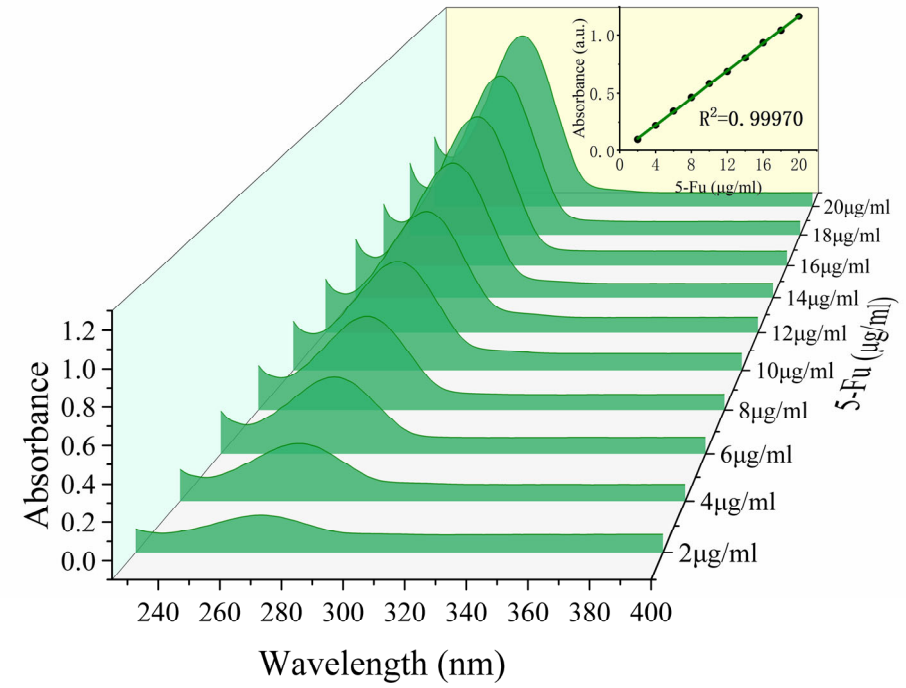

Figure S10 Standard curve of 5-Fu in ethanol solution

4. Encapsulation mechanism

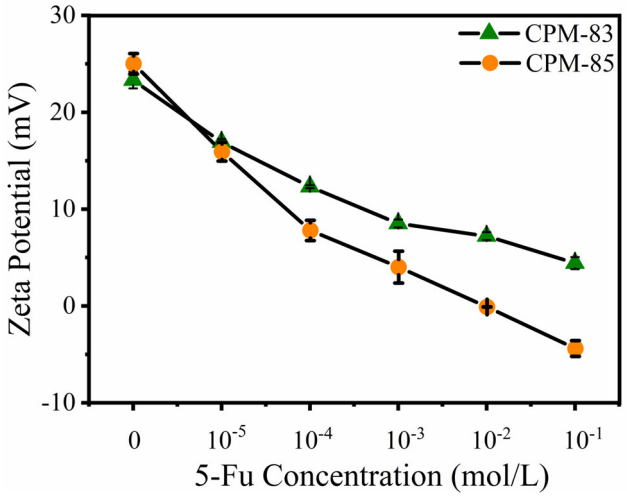

Figure S11 Zeta potential of CPM-83 and CPM-85 under different concentrations of 5-Fu

5. Kinetic model fitting

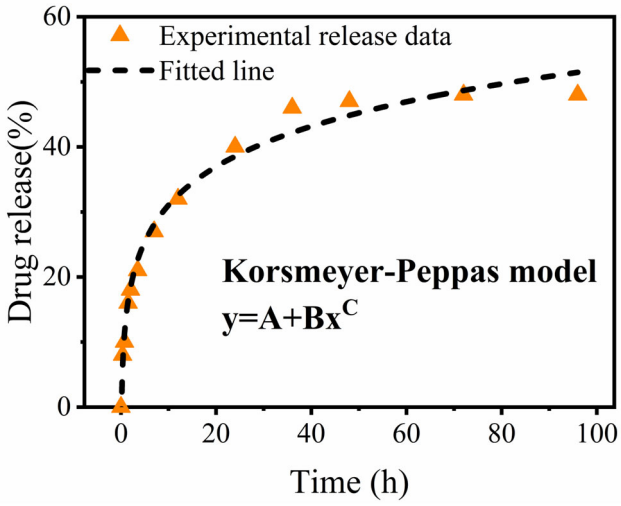

Figure S12 Pharmacokinetic simulation of 5-Fu@CPM-83 by Korsmeyer-Peppas model

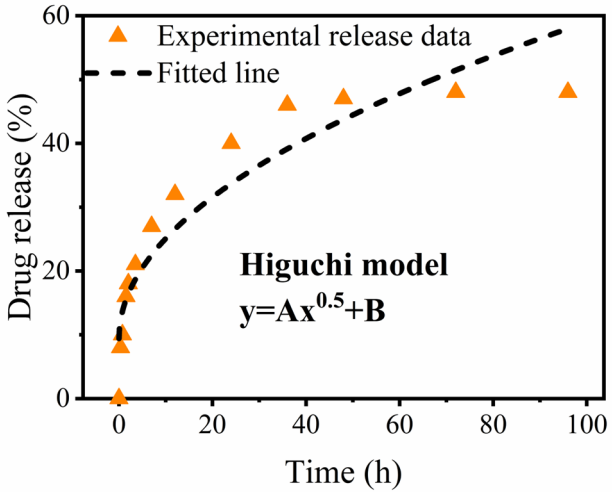

Figure S13 Pharmacokinetic simulation of 5-Fu@CPM-83 by Higuchi model

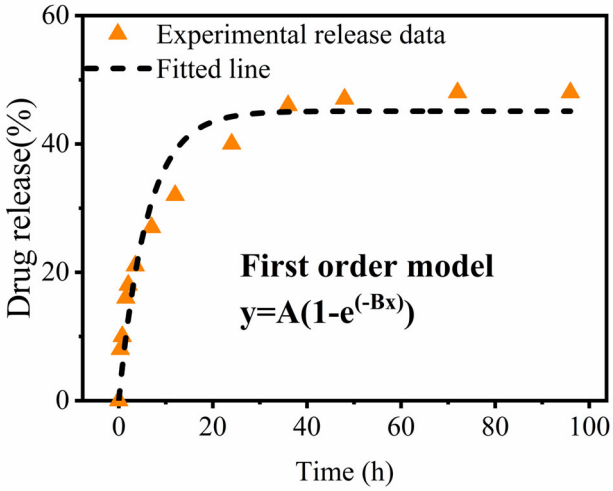

Figure S14 Pharmacokinetic simulation of 5-Fu@CPM-83 by first order model

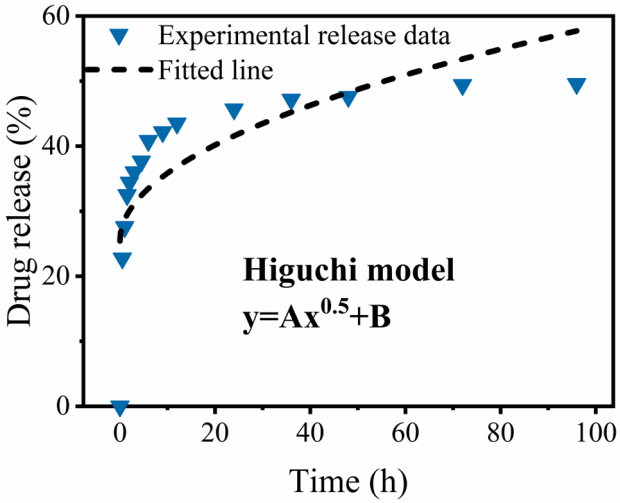

Figure S15 Pharmacokinetic simulation of 5-Fu@CPM-85 by Higuchi model

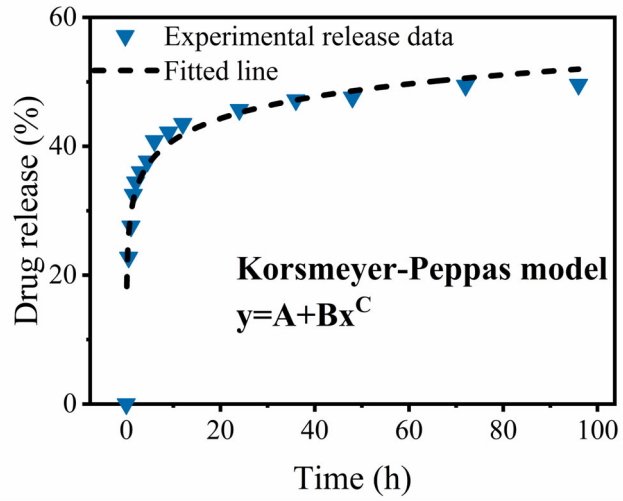

Figure S16 Pharmacokinetic simulation of 5-Fu@CPM-85 by Korsmeyer-Peppas model

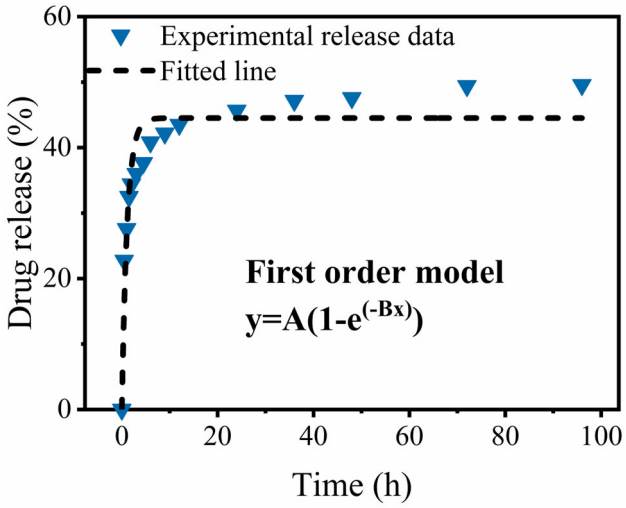

Figure S17 Pharmacokinetic simulation of 5-Fu@CPM-85 by first order model

Table S1 Summary of four types of kinetic model fitting tables for drug sustained release behavior under different pH conditions (5-Fu@CPM-83)

pH=7.4	Model	Fitted Equations	Correlation Coefficients(R^2)
First order		$y=0.45113(1-e^{-0.16551x})$	0.92938
Hill		$y=0.61664x^{0.6231}/(9.14866^{0.6231}+x^{0.6231})$	0.99237
Higuchi		$y=0.049556x^{0.5}+0.09407$	0.87759
Korsemeyer-peppas		$y=-0.85434+0.98826x^{0.07138}$	0.97917
pH=6.8	Model	Fitted Equations	Correlation Coefficients(R^2)
First order		$y=0.47509(1-e^{-0.23989x})$	0.92635

Hill		$y=0.62673x^{0.6339}/(9.14866^{0.6339}+x^{0.6339})$	0.99581
Higuchi		$y=0.05192x^{0.5}+0.11549$	0.85944
Korsemeyer-peppas		$y=-5.40825+5.5673x^{0.01479}$	0.98647
pH=1.5	Model	Fitted Equations	Correlation Coefficients(R^2)
First order		$y=0.69693(1-e^{-0.21149x})$	0.89666
Hill		$y=1.02327x^{0.55156}/(9.14866^{0.55156}+x^{0.55156})$	0.98905
Higuchi		$y=0.07634x^{0.5}+0.16602$	0.86854
Korsemeyer-peppas		$y=-1.73423+1.96659x^{0.05619}$	0.98447

Table S2 Summary of four types of kinetic model fitting tables for drug sustained release behavior under different pH conditions (5-Fu@CPM-85)

pH=7.4	Model	Fitted Equations	Correlation Coefficients(R^2)
First order		$y=0.78788(1-e^{-1.0485x})$	0.96695
Hill		$y=0.82685x^{1.05904}/(0.60126^{1.05904}+x^{1.05904})$	0.98849
Higuchi		$y=0.05185x^{0.5}+0.48279$	0.42684
Korsemeyer-peppas		$y=-257.490+258.048x^{2.9277E-4}$	0.78362
pH=6.8	Model	Fitted Equations	Correlation Coefficients(R^2)
First order		$y=0.76357(1-e^{-0.63296x})$	0.98019
Hill		$y=0.79895x^{1.1675}/(1.06502^{1.1675}+x^{1.1675})$	0.99455
Higuchi		$y=0.05877x^{0.5}+0.39575$	0.51102
Korsemeyer-peppas		$y=-1898.81+1899.26x^{5.145E-5}$	0.80863
pH=1.5	Model	Fitted Equations	Correlation Coefficients(R^2)
First order		$y=0.44505(1-e^{-0.89049x})$	0.90648
Hill		$y=0.52199x^{0.58313}/(0.74196^{0.58313}+x^{0.58313})$	0.99747
Higuchi		$y=0.03295x^{0.5}+0.2543$	0.54657
Korsemeyer-peppas		$y=-777.925+778.222x^{6.2757E-5}$	0.94960

6. Cell viability test

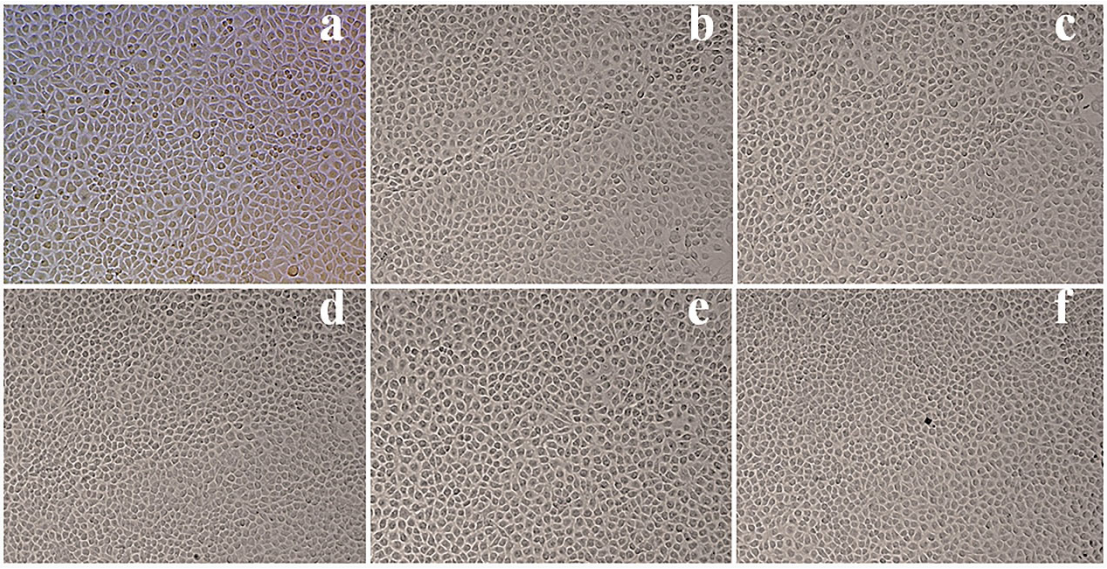

Figure S18 The L929 cell morphology after treated with different concentration of CPM-83, (a) Control，(b) 20μg/ml, (c) 40μg/ml, (d) 60μg/ml, (e) 80μg/ml, (f)100μg/ml

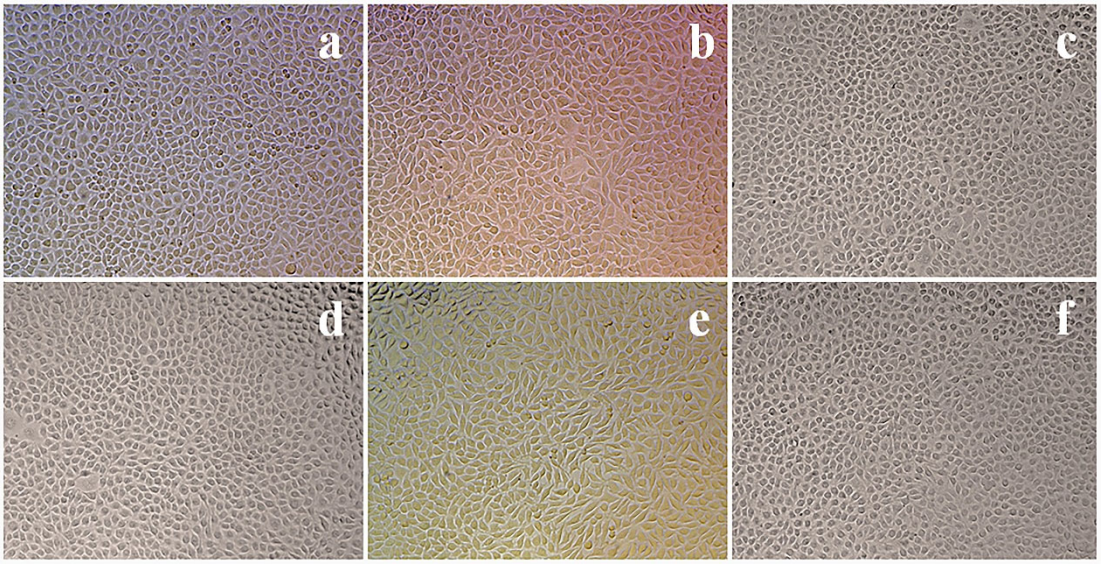

Figure S19 The L929 cell morphology after treated with different concentration of CPM-85, (a) Control，(b) 20μg/ml, (c) 40μg/ml, (d) 60μg/ml, (e) 80μg/ml, (f)100μg/ml

7. X-ray powder diffraction after drug release

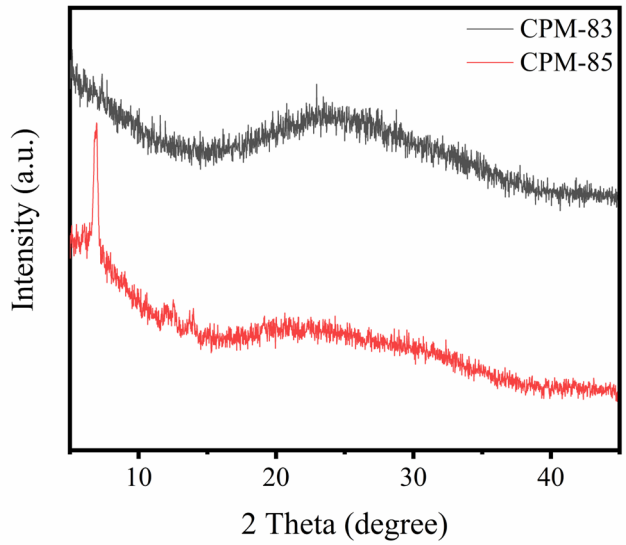

Figure S20 X-ray powder diffraction of CPM-83 and CPM-85 after drug release